

# Reproduction Quality Notice

This document is part of the Air Technical Index [ATI] collection. The ATI collection is over 50 years old and was imaged from roll film. The collection has deteriorated over time and is in poor condition. DTIC has reproduced the best available copy utilizing the most current imaging technology. ATI documents that are partially legible have been included in the DTIC collection due to their historical value.

If you are dissatisfied with this document, please feel free to contact our Directorate of User Services at [703] 767-9066/9068 or DSN 427-9066/9068.

**Do Not Return This Document  
To DTIC**

Reproduced by



CENTRAL AIR DOCUMENTS OFFICE

WRIGHT-PATTERSON AIR FORCE BASE - DAYTON, OHIO

REEL-C

3363 B

A.T.I

71048

*The*  
U.S. GOVERNMENT

IS ABSOLVED

FROM ANY LITIGATION WHICH MAY ENSUE FROM ANY  
INFRINGEMENT ON DOMESTIC OR FOREIGN PATENT RIGHTS  
WHICH MAY BE INVOLVED.

UNCLASSIFIED

*Reproduced*

FROM

LOW CONTRAST COPY.

ORIGINAL DOCUMENTS  
MAY BE OBTAINED ON  
LOAN

FROM

**CADDO**

FILE NO. 71048  
G. D. J. FILE COPY

**NATIONAL ADVISORY COMMITTEE  
FOR AERONAUTICS**

**REPORT No. 912**

**THE INTERDEPENDENCE OF VARIOUS TYPES OF  
AUTOIGNITION AND KNOCK**

**By H. LOWELL OLSEN and CEARCY D. MILLER**



**1948**

## AERONAUTIC SYMBOLS

### 1. FUNDAMENTAL AND DERIVED UNITS

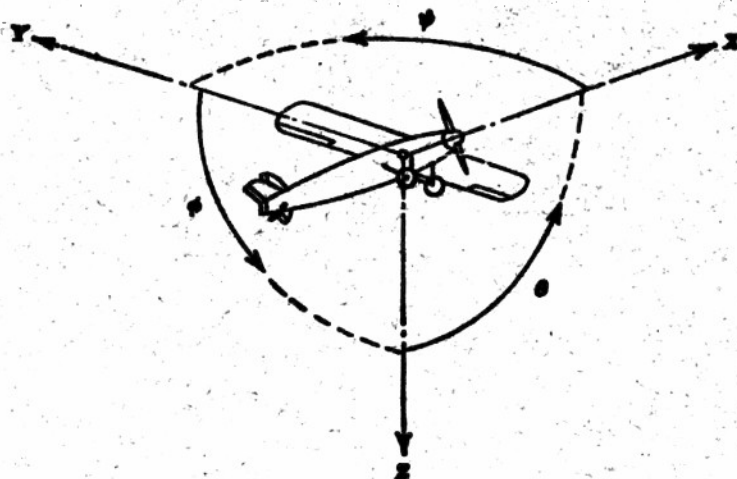
	Symbol	Metric		English	
		Unit	Abbreviation	Unit	Abbreviation
Length.....	<i>l</i>	meter.....	m	foot (or mile).....	ft (or mi)
Time.....	<i>t</i>	second.....	s	second (or hour).....	sec (or hr)
Force.....	<i>F</i>	weight of 1 kilogram.....	kg	weight of 1 pound.....	lb
Power.....	<i>P</i>	horsepower (metric)		horsepower.....	hp
Speed.....	<i>V</i>	(kilometers per hour.....)	kph	miles per hour.....	mph
		(meters per second.....)	mps	feet per second.....	fps

### 2. GENERAL SYMBOLS

<p><b>W</b> Weight = <math>mg</math></p> <p><b>g</b> Standard acceleration of gravity = <math>9.80665 \text{ m/s}^2</math> or <math>32.1740 \text{ ft/sec}^2</math></p> <p><b>m</b> Mass = <math>\frac{W}{g}</math></p> <p><b>I</b> Moment of inertia = <math>mk^2</math>. (Indicate axis of radius of gyration <math>k</math> by proper subscript.)</p> <p><b><math>\mu</math></b> Coefficient of viscosity</p>	<p><b><math>\nu</math></b> Kinematic viscosity</p> <p><b><math>\rho</math></b> Density (mass per unit volume)</p> <p>Standard density of dry air, <math>0.12497 \text{ kg-m}^{-3}\text{-s}^2</math> at <math>15^\circ \text{ C}</math> and <math>760 \text{ mm}</math>; or <math>0.002378 \text{ lb-ft}^{-3}\text{-sec}^2</math></p> <p>Specific weight of "standard" air, <math>1.2255 \text{ kg/m}^3</math> or <math>0.07651 \text{ lb/cu ft}</math></p>
--	--

### 3. AERODYNAMIC SYMBOLS

<p><b>S</b> Area</p> <p><b><math>S_w</math></b> Area of wing</p> <p><b>G</b> Gap</p> <p><b>b</b> Span</p> <p><b>c</b> Chord</p> <p><b>A</b> Aspect ratio, <math>\frac{b^2}{S}</math></p> <p><b>V</b> True air speed</p> <p><b>q</b> Dynamic pressure, <math>\frac{1}{2}\rho V^2</math></p> <p><b>L</b> Lift, absolute coefficient <math>C_L = \frac{L}{qS}</math></p> <p><b>D</b> Drag, absolute coefficient <math>C_D = \frac{D}{qS}</math></p> <p><b><math>D_0</math></b> Profile drag, absolute coefficient <math>C_{D_0} = \frac{D_0}{qS}</math></p> <p><b><math>D_i</math></b> Induced drag, absolute coefficient <math>C_{D_i} = \frac{D_i}{qS}</math></p> <p><b><math>D_p</math></b> Parasite drag, absolute coefficient <math>C_{D_p} = \frac{D_p}{qS}</math></p> <p><b>C</b> Cross-wind force, absolute coefficient <math>C_o = \frac{C}{qS}</math></p>	<p><b><math>i_w</math></b> Angle of setting of wings (relative to thrust line)</p> <p><b><math>i_s</math></b> Angle of stabilizer setting (relative to thrust line)</p> <p><b>Q</b> Resultant moment</p> <p><b><math>\Omega</math></b> Resultant angular velocity</p> <p><b>R</b> Reynolds number, <math>\rho \frac{Vl}{\mu}</math> where <math>l</math> is a linear dimension (e.g., for an airfoil of 1.0 ft chord, 100 mph, standard pressure at <math>15^\circ \text{ C}</math>, the corresponding Reynolds number is 935,400; or for an airfoil of 1.0 m chord, 100 mps, the corresponding Reynolds number is 6,865,000)</p> <p><b><math>\alpha</math></b> Angle of attack</p> <p><b><math>\epsilon</math></b> Angle of downwash</p> <p><b><math>\alpha_0</math></b> Angle of attack, infinite aspect ratio</p> <p><b><math>\alpha_i</math></b> Angle of attack, induced</p> <p><b><math>\alpha_a</math></b> Angle of attack, absolute (measured from zero-lift position)</p> <p><b><math>\gamma</math></b> Flight-path angle</p>
--	--



Positive directions of axes and angles (forces and moments) are shown by arrows

Axis		Force (parallel to axis) symbol	Moment about axis			Angle		Velocities	
Designation	Symbol		Designation	Symbol	Positive direction	Designation	Symbol	Linear (component along axis)	Angular
Longitudinal.....	X	X	Rolling.....	L	Y → Z	Roll.....	$\phi$	u	P
Lateral.....	Y	Y	Pitching.....	M	Z → X	Pitch.....	$\theta$	v	q
Normal.....	Z	Z	Yawing.....	N	X → Y	Yaw.....	$\psi$	w	r

Absolute coefficients of moment

$$C_l = \frac{L}{q b S}$$

(rolling)

$$C_m = \frac{M}{q c S}$$

(pitching)

$$C_n = \frac{N}{q b S}$$

(yawing)

Angle of set of control surface (relative to neutral position),  $\delta$ . (Indicate surface by proper subscript.)

#### 4. PROPELLER SYMBOLS

$D$  Diameter  
 $p$  Geometric pitch  
 $p/D$  Pitch ratio  
 $V'$  Inflow velocity  
 $V_s$  Slipstream velocity

$T$  Thrust, absolute coefficient  $C_T = \frac{T}{\rho n^3 D^4}$

$Q$  Torque, absolute coefficient  $C_Q = \frac{Q}{\rho n^3 D^5}$

$P$  Power, absolute coefficient  $C_P = \frac{P}{\rho n^3 D^5}$

$C_s$  Speed-power coefficient =  $\sqrt{\frac{C_P}{C_T}}$

$\eta$  Efficiency

$n$  Revolutions per second, rps

$\phi$  Effective helix angle =  $\tan^{-1} \left( \frac{V}{2\pi r n} \right)$

#### 5. NUMERICAL RELATIONS

1 hp = 76.04 kg-m/s = 550 ft-lb/sec

1 metric horsepower = 0.9863 hp

1 mph = 0.4470 mps

1 mps = 2.2369 mph

1 lb = 0.4536 kg

1 kg = 2.2046 lb

1 mi = 1,609.35 m = 5,280 ft

1 m = 3.2808 ft

---

**REPORT No. 912**

---

**THE INTERDEPENDENCE OF VARIOUS TYPES OF  
AUTOIGNITION AND KNOCK**

**By H. LOWELL OLSEN and CEARCY D. MILLER**

**Aircraft Engine Research Laboratory  
Cleveland, Ohio**

---

I

# National Advisory Committee for Aeronautics

*Headquarters, 1724 F Street NW, Washington 25, D. C.*

Created by act of Congress approved March 3, 1915, for the supervision and direction of the scientific study of the problems of flight (U. S. Code, title 50, sec. 151). Its membership was increased to 17 by act approved May 25, 1948. (Public Law 549, 80th Congress). The members are appointed by the President, and serve as such without compensation.

JEROME C. HUNSAKER, Sc. D., Cambridge, Mass., *Chairman*

ALEXANDER WETMORE, Sc. D., Secretary, Smithsonian Institution, *Vice Chairman*

HON. JOHN R. ALISON, Assistant Secretary of Commerce.

DETLEY W. BRONK, Ph. D., President, Johns Hopkins University.

KARL T. COMPTON, Ph. D. Chairman, Research and Development Board, National Military Establishment.

EDWARD U. CONDON, Ph. D., Director, National Bureau of Standards.

JAMES H. DOOLITTLE, Sc. D., Vice President, Shell Union Oil Corp.

R. M. HAZEN, B. S., Director of Engineering, Allison Division, General Motors Corp.

WILLIAM LITTLEWOOD, M. E., Vice President, Engineering, American Airlines, Inc.

THEODORE C. LONNQUEST, Rear Admiral, United States Navy, Assistant Chief for Research and Development, Bureau of Aeronautics.

EDWARD M. POWERS, Major General, United States Air Force, Assistant Chief of Air Staff-4.

JOHN D. PRICE, Vice Admiral, United States Navy, Deputy Chief of Naval Operations (Air).

ARTHUR E. RAYMOND, M. S., Vice President, Engineering, Douglas Aircraft Co., Inc.

FRANCIS W. REICHELDEFFER, Sc. D., Chief, United States Weather Bureau.

HON. DELOS W. RENTZEL, Administrator of Civil Aeronautics, Department of Commerce.

HOYT S. VANDENBERG, General, Chief of Staff, United States Air Force.

THEODORE P. WRIGHT, Sc. D., Vice President for Research, Cornell University.

HUGH L. DRYDEN, Ph. D., *Director of Aeronautical Research*

JOHN F. VICTORY, LL.M., *Executive Secretary*

JOHN W. CROWLEY, JR., B. S., *Associate Director of Aeronautical Research*

E. H. CHAMBERLIN, *Executive Officer*

HENRY J. E. REID, Eng. D., Director, Langley Aeronautical Laboratory, Langley Field, Va.

SMITH J. DEFRANCE, B. S., Director, Ames Aeronautical Laboratory, Moffett Field, Calif.

EDWARD R. SHARP, Sc. D., Director, Lewis Flight Propulsion Laboratory, Cleveland Airport, Cleveland, Ohio

## TECHNICAL COMMITTEES

AERODYNAMICS  
POWER PLANTS FOR AIRCRAFT  
AIRCRAFT CONSTRUCTION

OPERATING PROBLEMS  
INDUSTRY CONSULTING

*Coordination of Research Needs of Military and Civil Aviation*

*Preparation of Research Programs*

*Allocation of Problems*

*Prevention of Duplication*

*Consideration of Inventions*

LANGLEY AERONAUTICAL LABORATORY,  
Langley Field, Va.

LEWIS FLIGHT PROPULSION LABORATORY,  
Cleveland Airport, Cleveland, Ohio

AMES AERONAUTICAL LABORATORY,  
Moffett Field, Calif.

*Conduct, under unified control, for all agencies, of scientific research on the fundamental problems of flight*

OFFICE OF AERONAUTICAL INTELLIGENCE,  
Washington, D. C.

*Collection, classification, compilation, and dissemination of scientific and technical information on aeronautics*

## REPORT No. 912

### THE INTERDEPENDENCE OF VARIOUS TYPES OF AUTOIGNITION AND KNOCK

By H. LOWELL OLSEN and CEARCY D. MILLER

#### SUMMARY

*A study of the relations existing among pin-point autoignition, homogeneous autoignition, and knock has been made by means of the NACA high-speed camera and the full-view combustion apparatus. High-speed photographic records of combustion, together with corresponding pressure-time traces, of benzene, 2,2,3-trimethylbutane, S-4, and M-4 fuels at various engine conditions have shown the engine conditions under which each of these phenomena occur and the relation of these phenomena to one another.*

*Pin-point autoignition was encountered with benzene around the highest inlet-air temperatures and peak-compression pressures used. No homogeneous autoignition nor knock could be induced with benzene at any engine condition within the range of the apparatus. With 2,2,3-trimethylbutane, pin-point autoignition was encountered at high peak compression pressures with and without the occurrence of knock; no homogeneous autoignition was induced, but light knock did occur with and without pin-point autoignition. With S-4 fuel, all three phenomena were observed. The knock occurred alone at fairly low inlet-air temperatures and low compression pressures; at high inlet-air temperatures and high compression pressures, homogeneous autoignition occurred followed by violent knock; around the highest inlet-air temperatures and highest compression pressures within the range of the equipment, pin-point autoignition appeared followed by homogeneous autoignition, which, in turn, was followed by knock. Violent knock with S-4 in the presence of large unignited end zones was also observed. The M-4 reference fuel showed knock at relatively low inlet-air temperatures and peak compression pressures. At higher inlet-air temperatures and peak compression pressures, homogeneous autoignition of large extent and duration always followed by knock was observed. No pin-point autoignition was seen with M-4 fuel.*

#### INTRODUCTION

The general problem of spark-ignition-engine combustion and knock has been studied by the NACA for many years

and since 1939 a high-speed camera operating at the rate of 40,000 frames per second has been employed as a research tool in this study. This camera has produced considerable data on the knocking process and has made possible a more critical discussion of the various theories of spark-ignition engine knock. A description of normal combustion, pre-ignition, autoignition, and knock as shown by the high-speed camera is presented in references 1 to 5. Two of the conclusions reached in these references are: (1) The simple autoignition theory is inadequate as an explanation of spark-ignition engine knock; and (2) something resembling a detonation wave is associated with knock, as previously concluded by the Russian investigators Sokolik and Voinov (reference 6). The part played by the detonation wave in knock has been further illustrated by photographs taken with an ultra-high-speed camera at 200,000 frames per second (reference 7). As shown in reference 5, an adequate theory of knock must encompass both detonation and autoignition.

Several distinct types of autoignition have been shown to exist. The first type observed with the high-speed camera was the homogeneous autoignition presented in figure 5 of reference 1, which appears as a gradual change in optical properties of the entire end zone ahead of the advancing spark-ignited flames indicating the occurrence of spontaneous combustion in the end zone. A second type of autoignition is reported in figure 11 of reference 4, which shows the initiation of flames at discrete points in the end zone ahead of the advancing spark-ignited flames and was termed "pin-point autoignition." A third type, shown in figure 13 of reference 4, consists of the propagation of a regular autoignited flame front from the cylinder wall back toward the advancing spark-ignited flames.

Heretofore the occurrence of autoignition of any type has always been observed in the high-speed motion pictures to be followed by violent knock. The question whether knock must always follow autoignition arises from consideration of data presented by Woodbury, Lewis, and Canby (reference 8), Withrow and Boyd (reference 9), and others.

These data include photographs and pressure-time records of combustion that is described as knocking combustion. In these records a sharp pressure rise near peak pressure was interpreted as being caused by autoignition and also as being responsible for audible knock. These records showed no evidence of gas vibrations, which are now generally recognized as the usual feature of knock. An investigation of the interdependence of the various types of autoigniting and knocking combustion was therefore conducted to determine whether autoignition could be made to take place without the subsequent occurrence of the knocking reaction that gives rise to the gas vibrations. Engine conditions conducive to the occurrence of autoignition for several fuel types were consequently sought. The presence or absence of and the severity of the knock corresponding to these conditions were studied. No attempt was made at further explanation of the basic nature of the knocking reaction than has already been made in references 1 to 7.

The project, undertaken at the NACA Cleveland laboratory, involved the use of a full-view combustion apparatus (used for the first time in this investigation), the high-speed camera, and the pressure-recording apparatus. More than 300 shots of high-speed photographs and accompanying pressure-time traces were secured for a variety of fuels and engine operating conditions, and these data serve as the experimental foundation of the present report.

The experimental work of this investigation was completed in 1946.

#### APPARATUS AND PROCEDURE

The full-view combustion apparatus is a single-cylinder spark-ignition engine of  $4\frac{1}{8}$ -inch bore and 7-inch stroke. Figure 1 is a schematic diagram of the full-view combustion apparatus and the auxiliary equipment. The apparatus provides for photography of the whole combustion chamber through plate-glass windows that form the entire upper surface of the cylindrical combustion chamber. Schlieren photographs were taken of the contents of the combustion chamber. The optical system for the schlieren pictures included a concave stellite mirror mounted on top of the piston.

The jacket temperature was maintained at a set value by circulating heated ethylene glycol through the cooling passages of the cylinder head and the cylinder barrel. Combustion air at any desired pressure or temperature was continuously supplied to the intake port. The engine was brought up to speed by means of an electric motor and then operated under its own power for a single cycle by injecting a single charge of fuel from a special nozzle mounted in position A as shown in figure 1 (section M-M) and igniting this charge by four spark plugs in positions B, C, E, and F. The injection-advance angle and spark-advance angle were controlled by means of a sequence timing switch directly connected to the crankshaft. A single-cycle switch was placed in series with the sequence timing switch; the sequence timing switch was therefore effective only during the selected cycle for which the single-cycle switch was closed. Mechanically

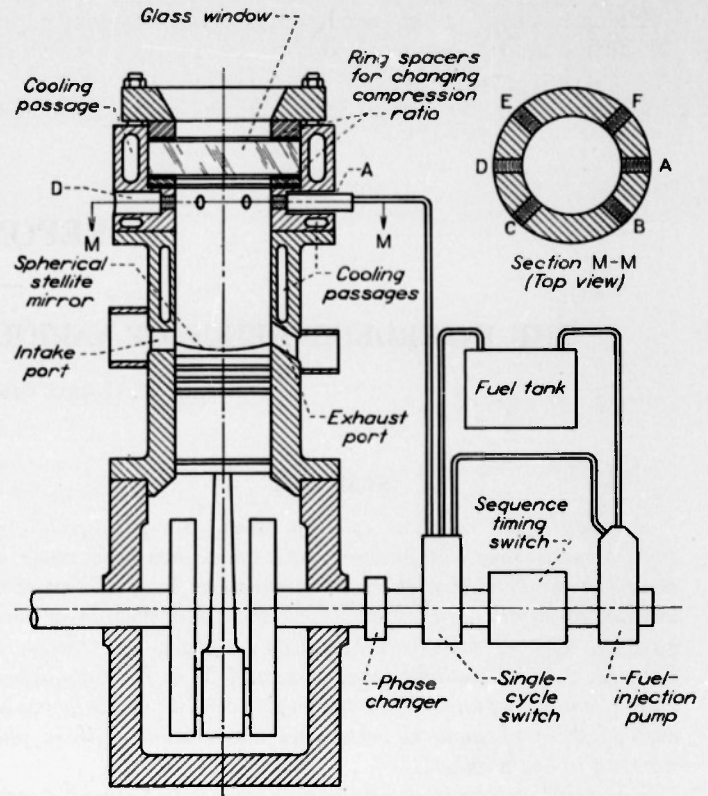


FIGURE 1.—Schematic diagram of full-view combustion apparatus.

ally connected to the single-cycle switch was a bypass valve in the output circuit of the fuel-injection pump. Through this valve the output of the fuel-injection pump returned to the fuel tank except when the single-cycle switch was closed, at which time a single charge of fuel was injected into the combustion chamber. The sequence timing switch also served to trip the high-speed camera shutter and the pressure-recording apparatus at the proper time with reference to the combustion.

The engine operating conditions held constant during the investigation were as follows:

Engine speed, rpm.....	500 ± 5
Jacket temperature, °F.....	240 ± 5
Fuel-injection-advance angle, degrees B.T.C.....	180 ± 5
Spark-advance angle, degrees B.T.C.....	19 ± 2

Other engine operating conditions were subject to variation for test purposes. The compression ratio was changed by using spacers of different thickness between the glass windows and the cylinder head. The intake-air pressure and temperature were controlled by means of reducing valves and an air heater, respectively, in the line from the laboratory combustion-air supply. The peak compression pressure was measured with a maximum-pressure gage, which replaced a spark plug before the actual run was made. The fuel-air ratio was controlled by adjusting the output of the fuel pump, but, because insufficient time was available for complete vaporization and mixing of the fuel, the ratio of fuel vapor to air in the burning charge is known only to a rough approximation.

The high-speed camera is fully described in reference 10. The optical system external to the camera was somewhat different from that previously used and is illustrated diagrammatically in figure 2. Light, originating at a source

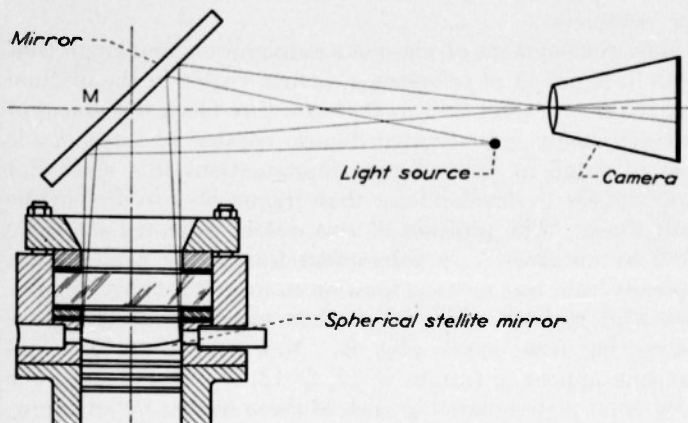


FIGURE 2.—Schematic diagram of optical system external to camera.

near the camera lens, was directed by mirror M into the combustion chamber to impinge on a concave stellite mirror fastened to the piston top. The stellite mirror reflected the light back to M and thence to the objective lens of the camera. The light source and camera objective lens were so placed that the spherical stellite mirror formed an image of the light source on the objective lens. The periphery of the objective lens acted as a schlieren stop and the entire optical system functioned as a schlieren system of low sensitivity. The light passing through the objective lens produced a schlieren photograph of the contents of the combustion chamber on the film in the high-speed camera. This optical system had the dual advantage of eliminating the need for a large, highly corrected schlieren lens and of eliminating piston-mirror breakage by substituting the durable stellite mirror for the glass mirrors formerly used in the work reported in references 1 to 5 and reference 7.

The pressure-recording apparatus utilized a quartz crystal piezoelectric pickup as the pressure-sensitive element; the pickup was mounted in the opening designated D in figure 1. The output from this pickup was fed into a very stable alternating-current amplifier whose frequency response is practically flat from 2 cycles per second to 30,000 cycles per second. The amplifier was specifically designed for this work and has been fully described by Krebs and Dallas (reference 11). The output from the amplifier was connected directly to the vertical deflection plates of a cathode-ray oscillograph tube; the vertical deflection of the light spot on the oscillograph screen was therefore made directly proportional to the pressure in the combustion chamber. The horizontal sweep circuit of the oscillograph was not used; an accurate linear time scale was established by using a rotating-drum camera driven by a synchronous motor, and focusing an image of the spot of light from the fluorescent screen on the film carried by the rotating drum. The pressure-time traces therefore have accurate vertical pressure scales and accurate horizontal time scales. The linear speed of the film carried past the

stationary light-spot image by the rotating drum was 500 inches per second.

The combustion apparatus, the camera, and the film drum were started at such times that the operating speeds of these instruments were reached nearly simultaneously. The single-cycle switch was then operated and, during the resulting power cycle, a high-speed motion picture and a pressure-time record of the combustion were obtained. This whole process is referred to as a "run."

#### PRESENTATION OF THE DATA

The data presented in this paper consist of seven high-speed motion pictures of combustion together with the corresponding pressure-time records (figs. 3 to 16), which are representative of a large amount of data. Certain features common to all the data will be pointed out before a detailed presentation is undertaken.

The high-speed motion pictures are presented as positive prints (figs. 3, 5, 7, 9, 11, 13, and 15). The individual frames are arranged in consecutive order in rows and columns beginning at the left end of the top row and terminating at the right end of the bottom row. The rows are lettered beginning at the top, and the columns are numbered beginning at the left; reference to any particular frame of the figure is accomplished by giving the row-letter and column-number appropriate to the frame in question. For example, the fourth frame in the second row is designated frame B-4, and so forth.

The positions of the spark plugs are marked in frame A-1 of each of figures 3, 5, 7, 9, 11, 13, and 15 by letters corresponding to the letters appearing in the combustion-chamber cross section of figure 1 (section M-M). These letters serve to orient the pictures with reference to the actual apparatus.

The pictures were taken by the schlieren method; therefore, in accordance with previous interpretations (reference 1), the dark mottled areas are believed to indicate regions of the charge in which combustion is in progress. The light area not yet reached in any particular frame by the mottled zones in their travel away from the spark-plug positions is interpreted as unignited charge; whereas the light areas behind the mottled zones are thought to indicate regions in which the burning is complete. The three small circular black spots appearing in every frame, except when obliterated by mottled zone, are caused by machine screws that hold the stellite mirror to the piston top. A ghost image, caused by an irregularity in the curve of the stellite mirror, appears near the center of the field of view as a bright spot when this region is covered by mottled zone. This ghost image is most clearly seen in row E of figure 5, but it is present in all the high-speed motion pictures presented and should be considered to have no relation to the combustion phenomena in the interpretation of the pictures.

The pressure-time records corresponding to the high-speed photographs are presented as positive projection prints (figs. 4, 6, 8, 10, 12, 14, and 16). The prints, like the original negatives, have linear vertical pressure scales and linear horizontal time scales, the deflection for a given pressure change being the same on each figure. In each record the

horizontal straight line is a reference line whose vertical position corresponds to the average cylinder pressure for the motoring cycle. The times of occurrence of ignition sparks and timing sparks are indicated by breaks in the traces. The time corresponding to the occurrence of the timing spark on the high-speed motion pictures is indicated by T on those figures where the timing spark occurred on the portion of the film presented (figs. 3 and 7). Other small breaks that occur on some of the pressure-time traces are caused by extraneous disturbances and are not combustion phenomena.

The operating conditions and results of the seven combustion runs are shown in table I. The knock intensity was determined by inspection of the maximum amplitude of the knocking vibration observed on the pressure trace. The pictures presented are representative of the combustion observed under the stated conditions. With the exception of figures 15 and 16, the pictures are also representative of the combustion occurring under the highest inlet-air temperature and peak compression pressures used for the various fuels. The highest values of the peak compression pressures and inlet-air temperatures used were limited, for benzene, 2,3,3-trimethylbutane, and S-4 fuels, by the strength of the apparatus and the capacity of the air heaters. The highest values of the peak compression pressures and inlet-air temperatures used for M-4 fuel were limited by the violence of the knock.

#### RESULTS AND DISCUSSION

High-speed motion pictures were taken of the combustion of benzene, 2,2,3-trimethylbutane, S-4, and M-4 fuels at engine conditions conducive to various types of autoignition and knock.

**Pin-point autoignition without knock.**—A high-speed motion picture of the combustion of benzene in the full-view combustion apparatus is shown in figure 3. The charge was ignited by four spark plugs placed at positions B, C, E, and F. Frame A-1 shows the position of the flames 93 frames after the time of ignition. The dark markings appearing at H in frame A-1 and in similar positions in succeeding frames are deposits of carbon on the stellite mirror from a previous run and should be disregarded. These dark markings are much intensified in frames A-9 to A-11. The reason for this intensification is unknown, but from A-12 on the spots appear the same as in A-1, showing that no real change occurred. The phenomena in the pictures that are interpreted as combustion phenomena exhibit a continuously changing visual aspect. The flames appear as roughly circular mottled bands spreading from centers at the spark-plug positions. The plugs were fired simultaneously, but the development of the flame marked C in frame A-1 is considerably retarded in comparison with the development of the other three flames, perhaps because of a locally lean or rich mixture ratio in the region H. The development of the flames after frame A-1 is readily visible. By frame F-10 flames had swept across the entire area of the combus-

tion chamber and the mottled region remaining in the frame indicates the portion of the charge that was still burning. Beyond frame F-10 the remaining mottled region slowly fades away; the last wisp disappears at about frame H-16 and the process of normal combustion is then considered to be complete.

The development of pin-point autoignition, similar to that seen in figure 11 of reference 4, is first visible in the original negatives in frames D-3 to D-6 as a tiny black dot ahead of the advancing spark-ignited flames; because of unavoidable loss of detail in the half-tone reproductions this black dot may appear to develop later than frames D-3 to D-6 in the half tones. The position of this dot is indicated in frame D-6 by an arrow. In subsequent frames the flame slowly spreads from this point of ignition to form a roughly circular patch of mottled zone, which then merges with the flame advancing from spark plug B. New pin points of autoignition appear in frames D-12, D-13, D-16, and E-3; the new point is designated in each of these frames by an arrow. Flame spreads from each of these points, eventually merging with either the spark-ignited flames or with other autoignited flames, until the whole end zone has been consumed. A measurement of the progress of the flame fronts shows that the velocity of the autoignited flames is very nearly the same as the velocity of the spark-ignited flames. From frame F-10 to frame H-16 the mottled region fades away gradually with no sign of an accelerated rate of reaction such as would accompany light knock. When figure 3 is projected as a motion picture, none of the characteristic gas vibration, which ordinarily accompanies knock with paraffin-type fuels, is visible. Figure 3 is therefore a picture of the occurrence of autoignition without the occurrence of the type of knock characterized by gas vibration.

Figure 4, the pressure-time record accompanying figure 3, shows no sign of knock and no indication of the occurrence of the autoignition. The increased over-all rate of burning caused by the autoignition is so slight that no visible evidence of it is apparent on the trace.

In the course of this investigation, 93 records of the combustion of benzene were obtained for a variety of peak compression pressures and inlet-air temperatures. Pin-point autoignition was obtained frequently at the highest inlet-air temperature and peak compression pressures allowable by the apparatus. No sign of the type of knock that gives rise to gas vibrations was detectable in any of the benzene runs.

**Pin-point autoignition with knock.**—Record of the occurrence of pin-point autoignition followed by light knock is presented in figure 5, which is a high-speed motion picture of the combustion of 2,2,3-trimethylbutane. Frame A-1 shows the configuration of the flames 129 frames after the ignition of the charge by four spark plugs. The dark markings appearing ahead of the flames in frame A-1 and persisting throughout most of the picture are a residue of carbon from a previous run and should be disregarded. The first evidence of pin-point autoignition is seen in frame B-5 as a dot pointed out by the arrow appearing in that frame. Addi-

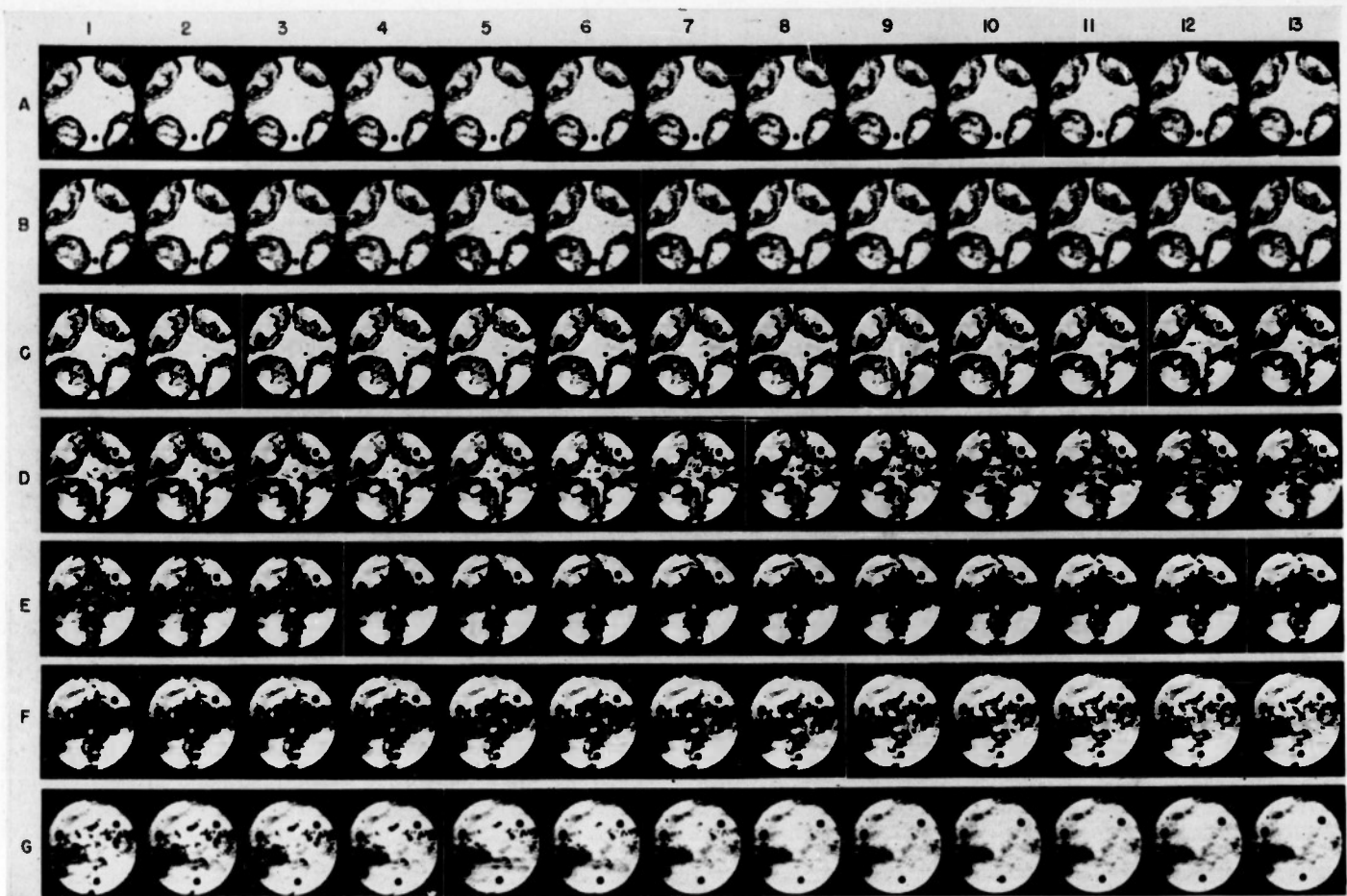


FIGURE 5.—High-speed motion picture of combustion of 2,2,3-trimethylbutane showing occurrence of pin-point autoignition followed by light knock.

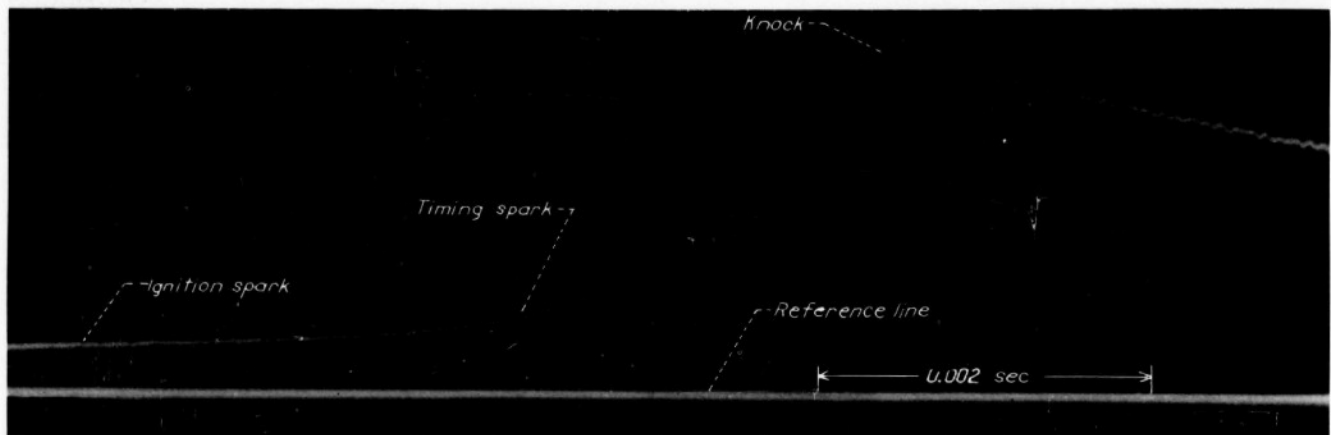


FIGURE 6.—Pressure-time record of combustion of 2,2,3-trimethylbutane corresponding to figure 5.

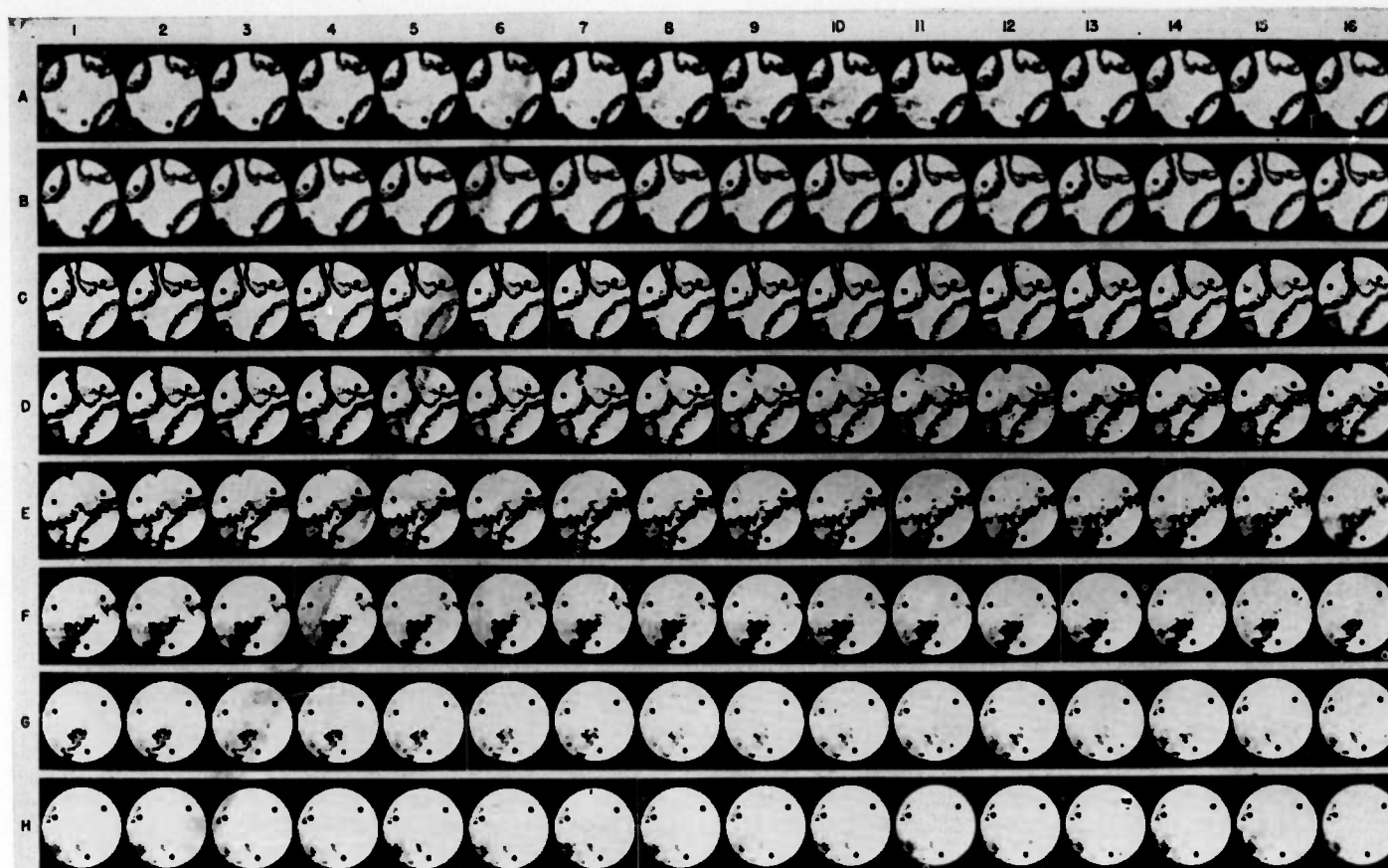


FIGURE 2.—High-speed motion picture of combustion of benzene showing occurrence of pin-point autoignition not followed by knock.

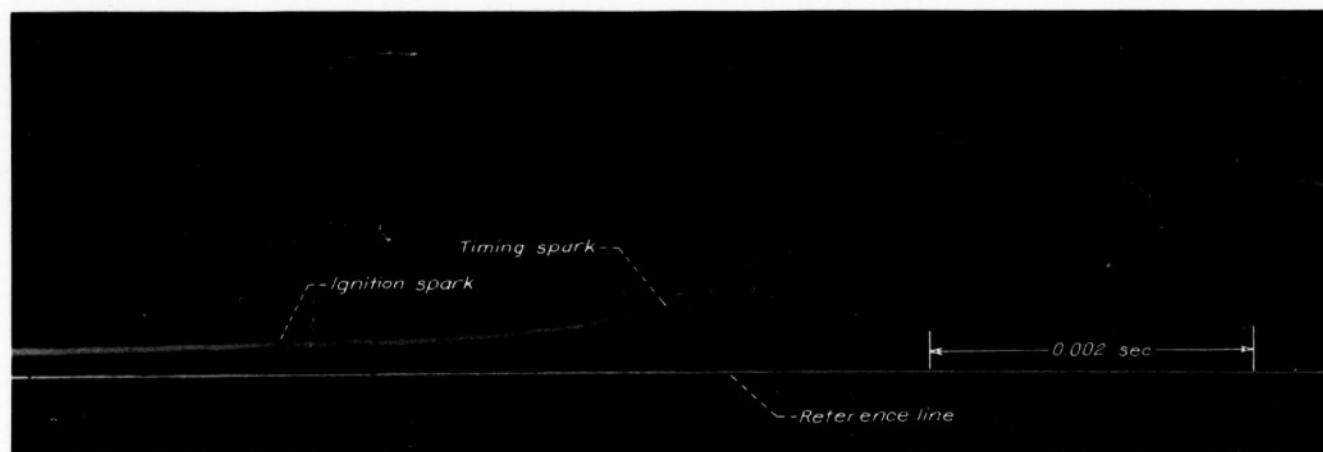


FIGURE 4.—Pressure-time record of combustion of benzene corresponding to figure 3.

tioned points of autoignition appear in frames B-11, C-7, C-12, D-1, D-3, D-7, and D-11, as indicated by the arrows. Flames spread slowly and evenly from each of these points until, by the time frame E-8 is reached, the end zone is completely consumed. By measurement of the flame fronts, the velocity of the autoignited flames was found to be approximately the same as the velocity of the spark-

ignited flames. From frame E-8 to frame G-8 the mottled region gradually fades away. An acceleration in the rate of decay of the mottled zone is apparent, however, in frames G-6 to G-8. This acceleration is the visual evidence of the occurrence of very light vibratory knock and is easily seen when the picture is projected on the motion-picture screen.

The pressure-time record for the combustion photographed in figure 5 is shown in figure 6. The trace shows the beginning of mild gas vibration due to knock, indicated in the figure, near the region of maximum pressure. As with benzene, no visible evidence of the occurrence of autoignition is seen on the trace.

Of the 32 records of the combustion of 2,2,3-trimethylbutane obtained in this investigation, 15 showed pin-point autoignition. Of these 15, some showed pin-point autoignition followed by light vibratory knock similar to that of figure 5 and others showed pin-point autoignition without knock. No homogeneous autoignition was observed with 2,2,3-trimethylbutane. Limitations imposed by the apparatus prevented use of inlet-air temperatures and peak compression pressures sufficiently high to produce violent knock with 2,2,3-trimethylbutane.

Another example of the occurrence of pin-point autoignition followed by knock is presented in figure 7, which is a high-speed motion picture of the combustion of S-4 reference fuel. Frame A-1 was exposed 100 frames after the ignition of the charge by four spark plugs. The early development of the two right-hand flames is obscured by the dark region, resulting from poor schlieren illumination of the stellite mirror, extending across the right-hand portion of the field of view. The configurations of all four spark-ignited flames become clear, however, in row C. The first evidence of pin-point autoignition becomes visible in frames B-8 to B-11 as a very small black dot and is indicated by the arrow in frame B-11. Subsequent points of autoignition appear in frames C-3, C-7, D-11, E-1, and E-8 as indicated. As with the two previous examples, flames spread from these ignition points at normal flame speed. By the time frame E-8 is reached, a considerable fraction of the combustion-chamber volume has been swept through by autoignition flames, but a relatively large end zone remains in which the charge has not yet been ignited either by spark-ignited flame or by autoignition. In frame E-9 the entire end zone darkens slightly as if autoignition began to occur simultaneously throughout its entire volume. In the same frame there appears a characteristic blurring of the right-hand side of the chamber such as was shown in reference 3 to accompany knock. This blur is readily recognized by comparing corresponding parts of frames E-8 and E-9. The next frame shows evidence of an exceedingly violent knock, and the mottled zone is completely obliterated by frame E-11. During the frames of row F, a considerable amount of dense smoke was released by the knocking reaction; this smoke is designated by the letter S in frame F-3. The extremely rapid frame-to-frame changes in the configuration of smoke and luminous gases seen in the frames of row F were caused by the violent swirling and bouncing of the gases, as may be clearly seen when the frames are projected on a screen as a motion picture. Some deflection of the stellite mirror on the piston top occurs because of local high-pressure regions, and the

rapid frame-to-frame changes probably are partly caused by this deflection.

Figure 8 is the pressure-time record for the combustion process photographed in figure 7. As on the previous pressure records, there is no visual evidence of the occurrence of autoignition on the terrace, although the rate of pressure rise must undoubtedly be affected by the autoignition. Knock occurred at a point indicated on the trace at which the rapid pressure fluctuations begin. The knock is exceedingly violent as may be judged by the magnitude of the pressure fluctuations. The pressure amplitude of the knocking vibration is more than twice as great as the total pressure rise caused by the combustion prior to knock.

In the 87 records of the combustion of S-4 reference fuel obtained in this investigation, pin-point autoignition appeared when the inlet-air temperatures and peak compression pressures were near the highest obtainable with the apparatus and was invariably followed by a slight homogeneous autoignition, which in turn was followed by a violent knock.

From a visual standpoint, the pin-point autoignition shown in figures 3, 5, and 7 is remarkably similar. The autoignited flames are indistinguishable from spark-ignited flames except for origin and extent. The flame speed of the autoignited flames seems to be the normal flame speed prevailing at the time the autoignitions occur. The first point of autoignition appears fairly early in the combustion with the subsequent appearance of additional points of autoignition at apparently random times and places up to the time the whole end zone is inflamed. The increased rate of pressure rise caused by the appearance of pin-point autoignition is brought about so gradually that no irregularity in the pressure rise, such as might cause an audible sound in a running engine, is produced. The occurrence of pin-point autoignition appears to constitute an extension of normal burning such as would result from firing additional spark plugs at the location and times of inception of the points of autoignition.

The reason for the appearance of autoignition at the particular points observed is not clear, although a number of possibilities can be suggested. A first possibility is that, because the fuel and air are not thoroughly mixed, the ignition occurs in the regions possessing the fuel-air ratio most likely to ignite at the particular temperature and pressure encountered. A second possibility is that the autoignition occurs on particles suspended in the end gas, which serve as points of ignition. Such particles might be carbon, liquid fuel, oil, or atmospheric dust; and ignition could probably be caused by thermal or catalytic action on the surface of the particles.

**Homogeneous autoignition with knock.**—A high-speed motion picture of the combustion of M-4 reference fuel is shown in figure 9. Frame A-1 was taken 219 frames after the ignition of the charge. Only three flames appear; no burning resulted from the spark plug at F. The slow prog-

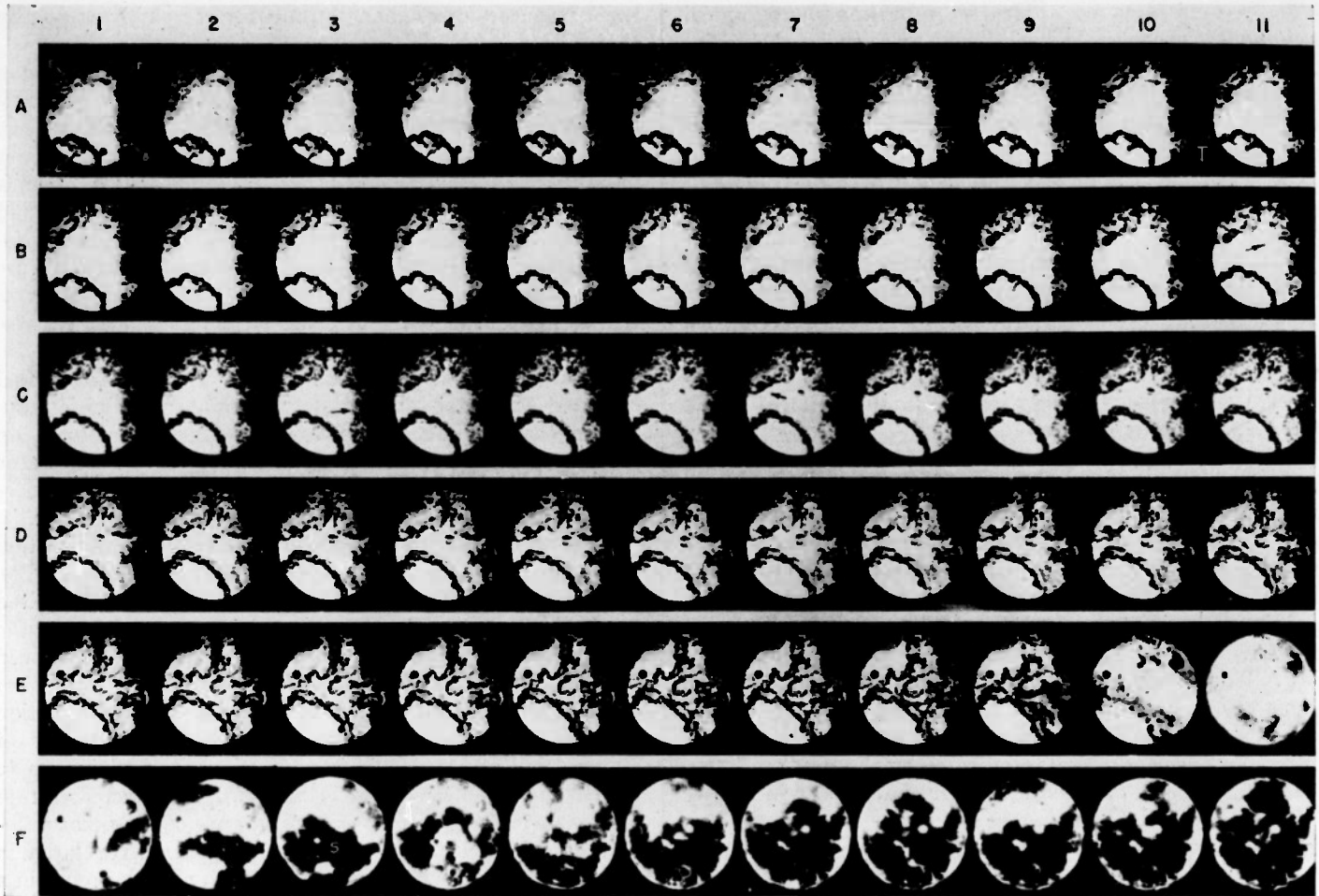


FIGURE 7.—High-speed motion picture of combustion of 8-4 reference fuel showing pin-point autoignition followed by violent knock.

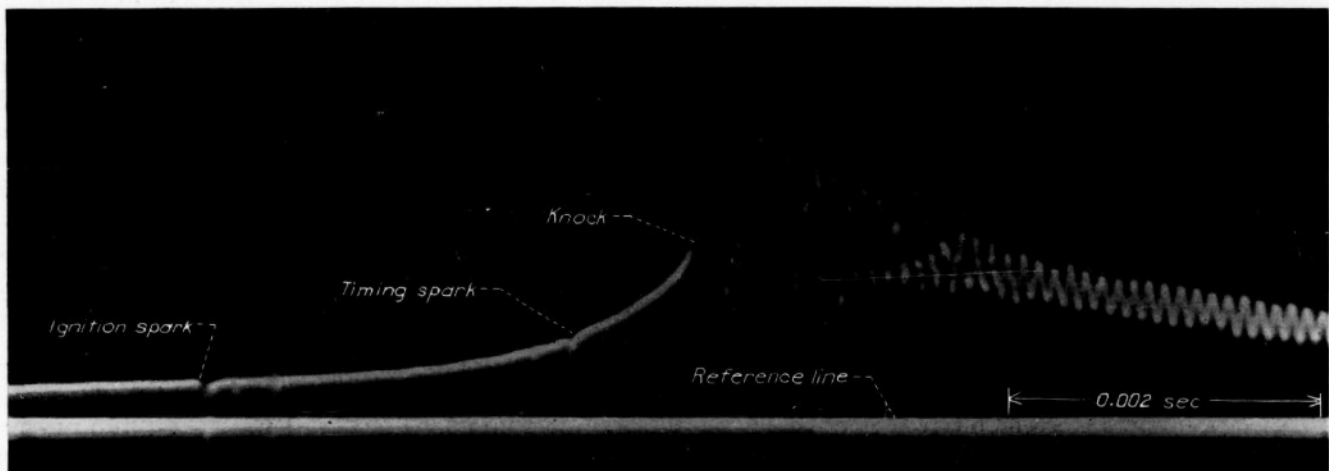


FIGURE 8.—Pressure-time record of combustion of 8-4 reference fuel corresponding to figure 7.

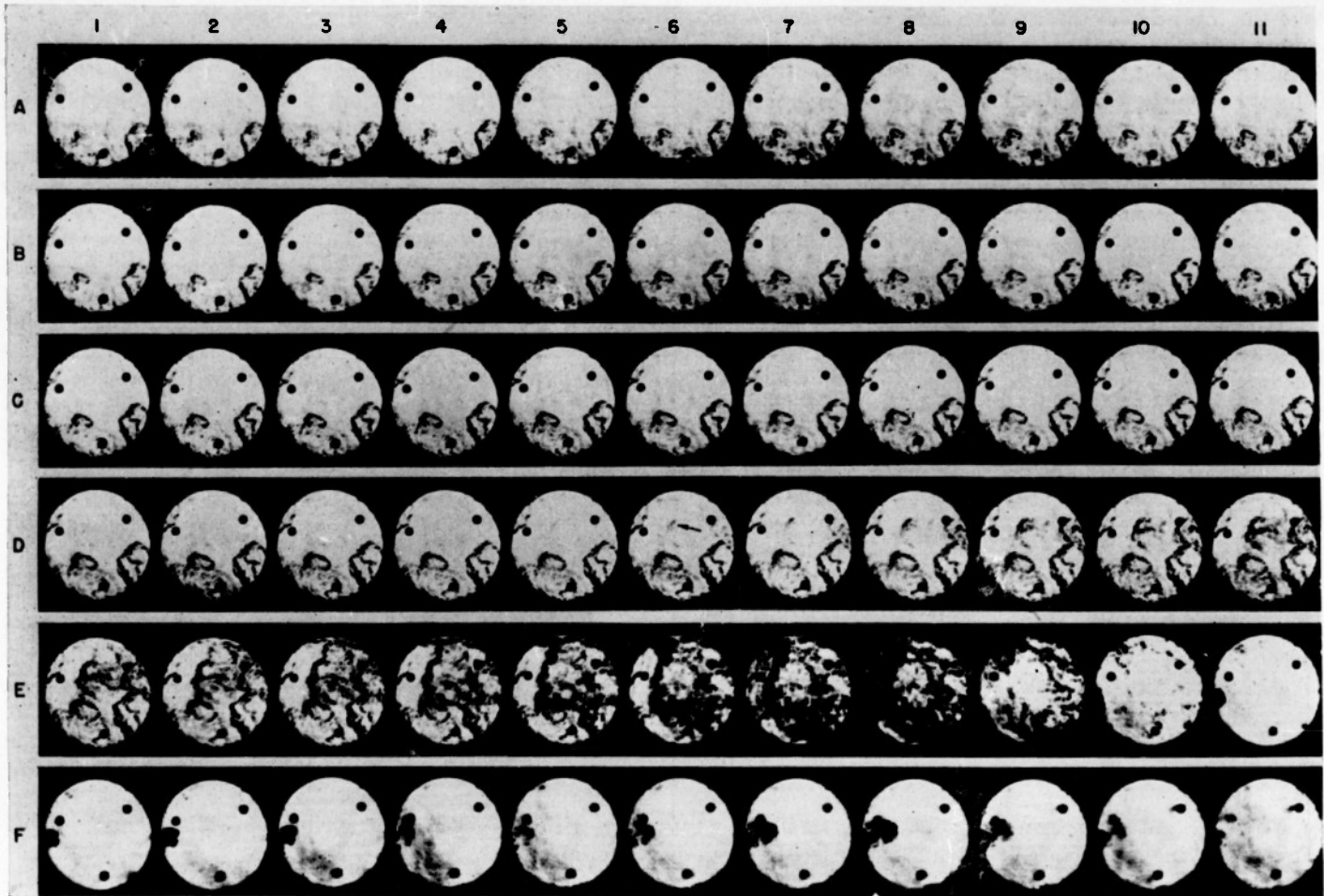


FIGURE 9.—High-speed motion picture of combustion of M-4 reference fuel showing extensive development of homogeneous autoignition followed by violent knock.

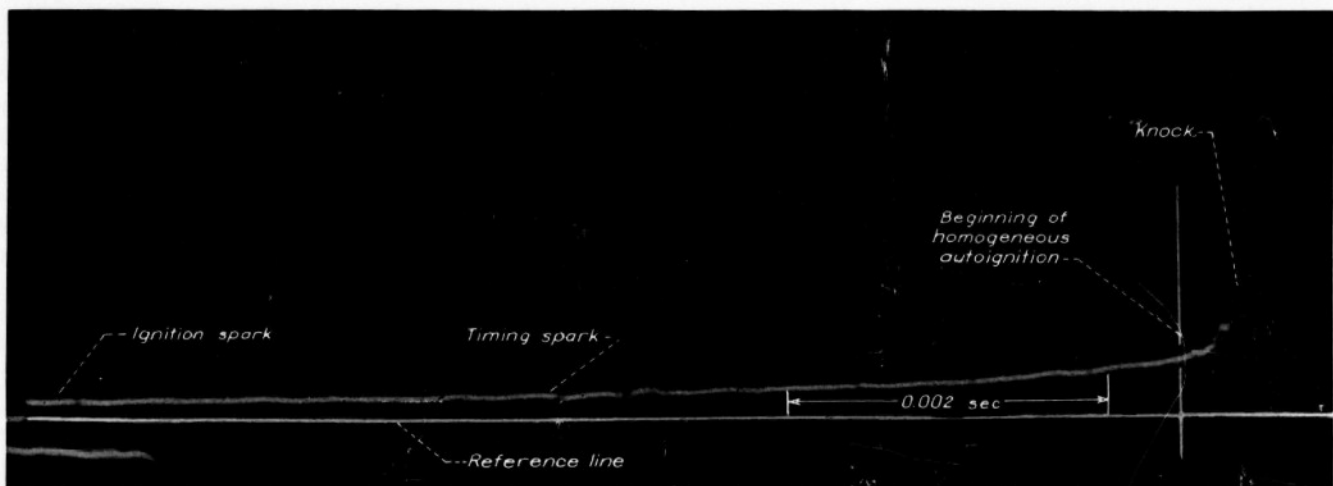


FIGURE 10.—Pressure-time record of combustion of M-4 reference fuel corresponding to figure 9.

ress of the three flames toward the center of the combustion chamber is readily apparent in rows A through C. The first evidence of autoignition appears as a dark region pointed out by the arrow in frame D-6. In the following frames this dark region grows rapidly in extent, not by a regular propagation of flame from the initial darkened region, but by the gradual appearance of additional darkened areas near, but not intimately connected with, the first darkened region. By the time frame E-2 is reached, burning is in progress throughout most of the combustion-chamber volume. The unflamed gas is confined to the remaining white region on the left-hand side of the field of view with its entire right-hand extremity formed by an autoignited flame front. In frames E-2 to E-6 this autoignited flame front moves toward the left with a speed considerably greater than the normal flame speed. In frames E-6 to E-8 a secondary homogeneous autoignition occurs throughout the entire remaining volume of unflamed gas. This secondary homogeneous autoignition closely resembles the less extensive homogeneous autoignition seen in references 1 and 2. A violent knock took place after the exposure of frame E-8 and the entire mottled region was cleared away in the next two frames. A quantity of smoke appears in the end zone immediately after knock. Very rapid changes in the configuration of the smoke in frames E-10 and E-11 and the frames of row F indicate the violent swirling and vibration of the gas set up by the knock.

The pressure-time record accompanying the combustion process shown in figure 9 is presented in figure 10. The trace shows that the rate of pressure rise was very small except during a short interval before knock. If frame E-9 of figure 9 is taken as the time of knock, then the time of exposure of frame D-6 is indicated on the pressure trace by the vertical line marked "beginning of homogeneous autoignition." Several rapid increases in the rate of pressure rise are seen between the vertical line and the knock. These increases in rate of pressure rise probably correspond to the increased rate of burning caused by the several homogeneous autoignitions.

Another illustration of the occurrence of homogeneous autoignition with M-4 reference fuel is shown in figure 11. Frame A-1 was taken 169 frames after the ignition of the charge. The first evidence of homogeneous autoignition occurs in frame C-1 in the general region indicated by the arrow. The autoignition rapidly appears in other regions in subsequent frames until in frame E-1 the entire field of view is covered by mottled zone, and apparently the whole cylinder charge is aflame either by autoignition or by spark ignition. The gas in the chamber continues to burn until about frame E-9 when knock takes place. The mottled region is completely cleared by frame F-4, whereas subsequent frames show the development of considerable smoke, especially near the edge of the combustion chamber.

The pressure-time record corresponding to figure 11 is given in figure 12. The knock is indicated on the trace and is taken to correspond in time to frame E-9. The vertical line, termed "beginning of homogeneous autoignition," corresponds in time to the beginning of autoignition in frame C-1. No rapid change in rate of pressure rise occurs until about the time indicated on the pressure trace, which corresponds approximately to frame E-1. The effect of the autoignition from frame C-1 to E-1 is therefore very small, but from E-1 to the time of knock the autoignition increases the rate of pressure rise manyfold.

The justification for selection of frame E-9 as the point of knock in figures 9 and 11 may not be apparent to an inexperienced observer. For both figures the selection was made partly on the basis of the extremely rapid frame-to-frame disintegration of the mottled combustion zone that is seen in comparison of frame E-8 with frame E-9, frame E-9 with frame E-10, frame E-10 with frame E-11, and so on. No comparably rapid disintegration of the mottled combustion zone can be seen in a comparison of frame E-7 with frame E-8 or frame E-6 with frame E-7, or in comparison of any two successive frames preceding frame E-6. The selection was further based on observation of the photographs as motion pictures on a screen, which indicated that the vibration of the gases is set up at frame E-9 in each case. The dependability of this method of selecting the point of knock relative to the high-speed photographs was shown in reference 3. In that reference the motion-picture frame selected by this method was shown to coincide chronologically with the onset of gas vibrations within one motion-picture frame.

The appearance of mottled regions in the end gas a considerable time in advance of the increased rate of pressure rise on the pressure trace, as shown in figure 11, is in harmony with the idea that the combustion process takes a relatively long time for its completion. This idea was advanced in reference 3, wherein, for normal combustion, the pressure rise was shown to continue as long as any of the mottled zone was apparent. The autoignited burning shown in frames C-1 to E-1 of figure 11 apparently represents the initial stages of the combustion process in which sufficient heat is released to set up detectable temperature gradients, but no appreciable pressure rise results from the release of this heat. From frame E-1 on, however, the autoignited combustion has reached a sufficiently advanced stage that the heat released from it is enough to effect the rate of pressure rise appreciably. The pressure is evidently still rising rapidly at the time the knock occurs at approximately frame E-9, thus indicating that the combustion is not completed at the time of the knock.

A comparison of figures 10 and 12 shows that the pressure-time records have very similar pressure profiles up to the time of knock. The autoignition of figure 11 is in progress for

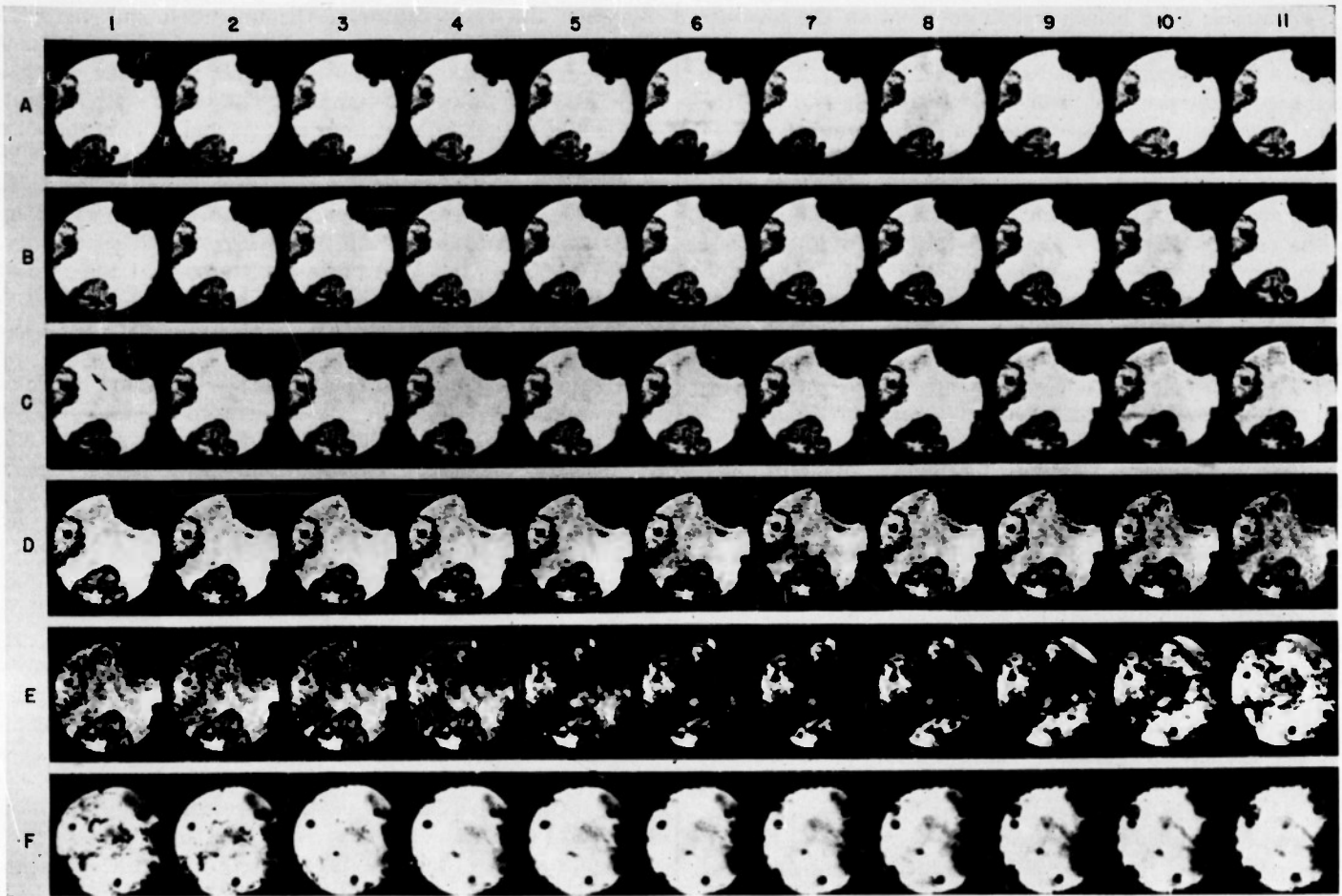


FIGURE 11.—High-speed motion picture of combustion of M-4 reference fuel showing extensive homogeneous autoignition followed by heavy knock.

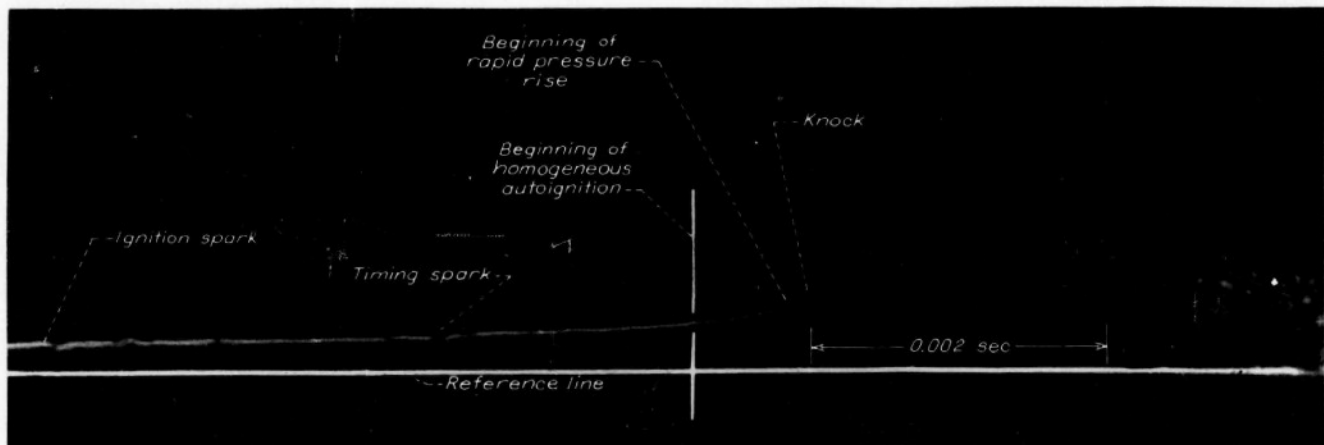


FIGURE 12.—Pressure-time record of combustion of M-4 reference fuel corresponding to figure 11.

a considerable time before a definite effect on the pressure trace is visible, whereas the autoignition of figure 9 affects the pressure trace almost immediately upon its inception. The similarity of the pressure profiles, however, suggests that the actual combustion processes represented by figures 9 and 11 are similar. The apparent differences in the two pictures might be explained as being caused by uncontrollable changes in the apparatus. Both the total amount of light passing to the camera and the schlieren sensitivity of the optical system are subject to some variation from one photograph to another because of the small uncontrolled motions of the stellite mirror on the moving piston top. The schlieren sensitivity and exposure of figure 11 might have been sufficiently different from those of figure 9 to allow the detection of considerably smaller temperature gradients in figure 11. The autoignition photographed in figure 11 is apparently seen in an earlier stage of combustion than that photographed in figure 9. In figure 9, combustion in the autoignited zone becomes visible only when the rate of heat release has become large enough to affect the general pressure rise; any autoigniting combustion process prior to this was undetected.

The engine conditions under which such extensive homogeneous autoignition with M-4 fuel appears are high inlet-air temperatures and high peak compression pressures. The fact that no pin-point autoignition appeared is apparently attributable to the chemical structure of the fuel. With inlet-air temperatures of 400° F and over and peak compression pressures of 190 pounds per square inch absolute and over, 13 of the 16 records exhibited extensive homogeneous autoignitions similar to those shown in figures 9 and 11.

The only fuel of the four used with which the homogeneous autoignition appeared in great extent was M-4 reference fuel. Homogeneous autoignition was definitely observed with S-4 reference fuel, but never appeared more than four motion-picture frames in advance of knock. No homogeneous autoignition was observed with either benzene or 2,2,3-trimethylbutane. It seems likely that S-4 fuel would show more extensive homogeneous autoignition under higher inlet-air temperatures and peak compression pressures than those used, and perhaps the other two fuels might also show homogeneous autoignition under much higher peak compression pressures and inlet-air temperatures.

The reason for the occurrence of homogeneous autoignition is probably the same as the reason originally postulated to account for knock on the simple autoignition theory. That

is, when the temperature of the unignited end gas rises above the ignition temperature because of adiabatic compression, spontaneous combustion is set up in the end gas after an appropriate ignition lag. The effect of this simultaneous combustion throughout a large end zone is to cause an appreciable increase in the rate of pressure rise. The increased rate of pressure rise, however, is not sufficient to cause the pressure fluctuation accompanying the knocking reaction, as is evident from figure 10. The discontinuity, which occurs at the time of knock, shows that the rate of pressure rise resulting in the gas vibrations is very much greater than the greatest rate of pressure rise caused by the preceding stages of autoignition.

Figure 13 is thought to be a high-speed motion picture of the combustion of a blend of M-4 reference fuel and benzene obtained under very high inlet-air temperature and peak compression pressure. After all the M-4 pictures had been taken, the M-4 fuel was removed from the fuel system and replaced with benzene and the peak compression pressure was increased to a value calculated to produce pin-point autoignition in the benzene. When the engine was fired, however, the violent knock shown in figures 13 and 14 took place. Some M-4 fuel was probably trapped in the fuel-injection nozzle and was responsible for the knocking combustion. Subsequent shots gave the characteristic normal burning of benzene. Figure 13 therefore represents the combustion of either M-4 reference fuel, or a blend of M-4 reference fuel and benzene, at considerably higher inlet-air temperature and peak compression pressure than had been intended (table I).

Frame A-1 was taken approximately 1325 microseconds after the ignition of the charge by four spark plugs, a time interval equivalent to that covered by 53 frames. All the frames reproduced in figure 13 were exposed while the camera shutter was in the process of opening; the first few frames of row A were the first frames to be exposed on the film. An inspection of frame A-7, at least on the original negative, shows that the flame from each of the four spark plugs had already become visible, the flame at position F being the most developed and the flame at position E being least developed. In frames B-1 to C-1 a dark cloud developed near the flame at position B and spread very rapidly and regularly throughout the combustion chamber. When the pictures are observed on the motion-picture screen, the nd-

TABLE I  
OPERATING CONDITIONS AND RESULTS OF AUTOIGNITION AND KNOCK TESTS

High-speed motion picture and corresponding pressure-time trace	Fuel	Timing spark (deg B. T. C.)	Ignition spark (deg B. T. C.)	Inlet-air temperature (°F)	Inlet-air pressure (lb/sq in. absolute)	Compression ratio	Peak compression pressure (lb/sq in. absolute)	Knock intensity	Type of autoignition
Figs. 3, 4	Benzene	12	21	425	15.6	9.0	340	None	Pin-point
Figs. 5, 6	2,2,3-Trimethylbutane	10	18	312	20.2	9.0	472	Very light	Do.
Figs. 7, 8	S-4	10	18	446	15.6	9.0	340	Very heavy	Pin-point and homogeneous
Figs. 9, 10	M-4	-----	21	398	14.3	7.0	190	Heavy	Homogeneous
Figs. 11, 12	M-4	-----	20	445	14.3	7.9	225	do.	Do.
Figs. 13, 14	M-4 Benzene	12	18	415	14.7	9.0	320	Very heavy	Do.
Figs. 15, 16	S-4	10	18	310	14.5	9.0	315	Heavy	None

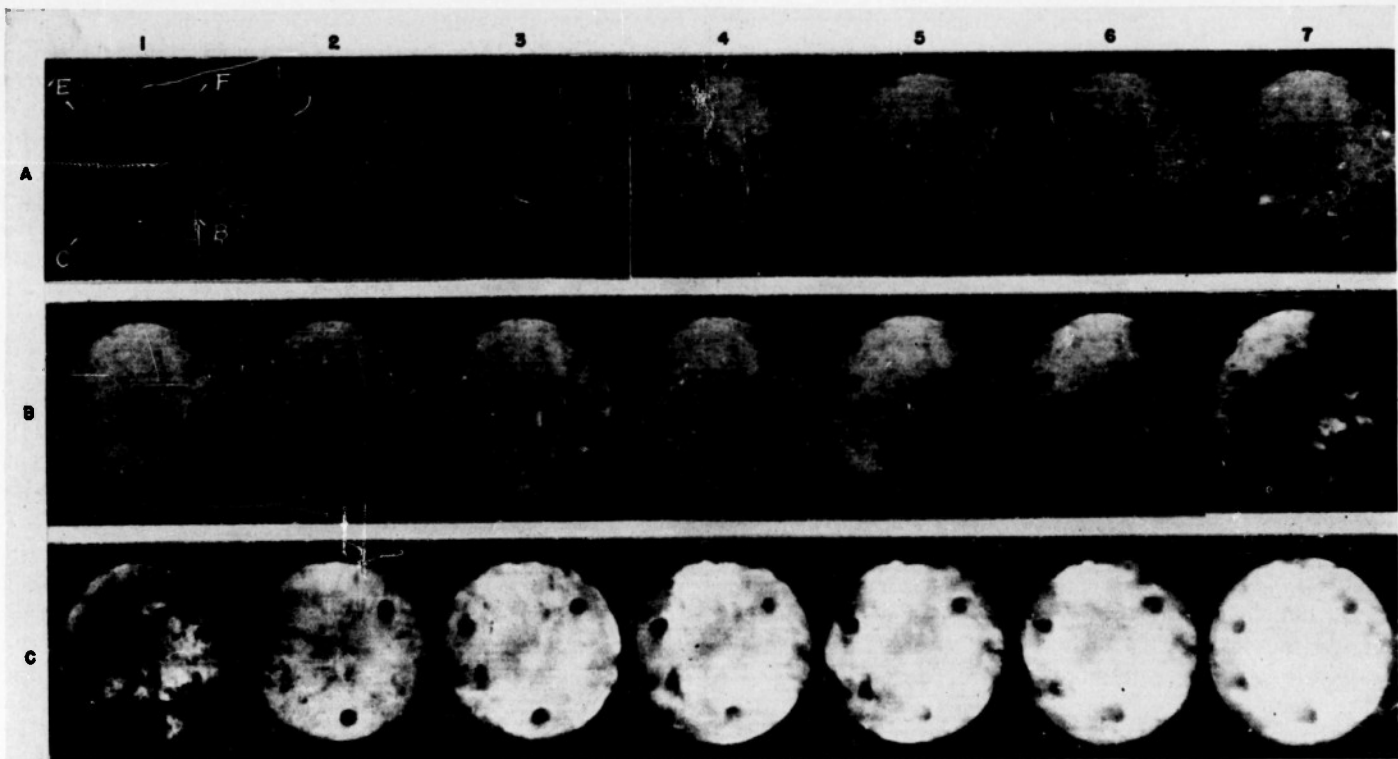


FIGURE 13.—High-speed motion picture of combustion of M-4 reference fuel under extremely severe engine conditions showing propagated homogeneous autoignition and severe knock.

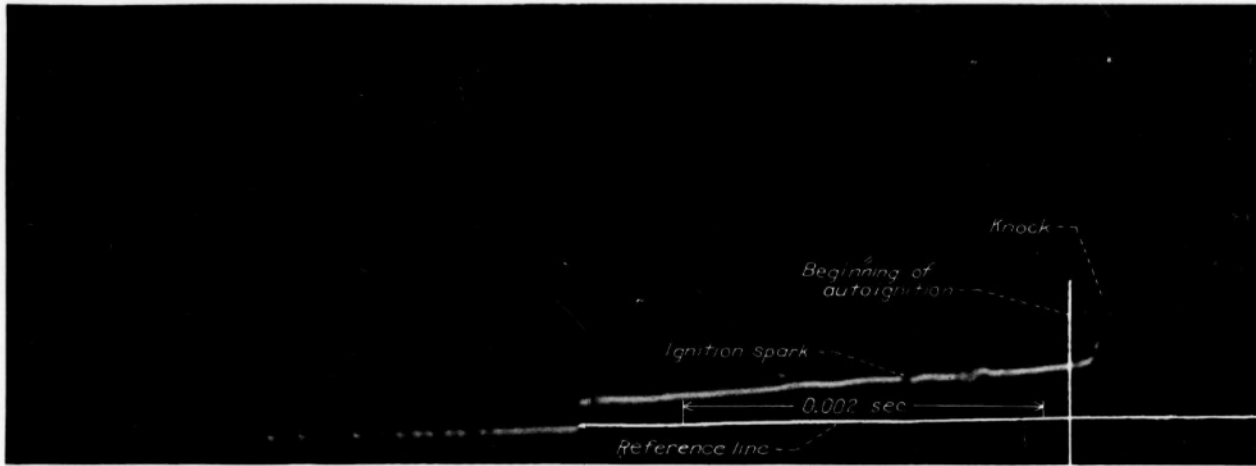


FIGURE 14.—Pressure-time record of combustion of blend of M-4 reference fuel and benzene corresponding to figure 13. Unusually severe engine conditions prevailing.

vance of the dark cloud has every appearance of a spatially progressive flame propagated at an extremely high speed throughout the combustion chamber and the violent bouncing of the gases initiated by knock is seen to begin immediately after this flame has completed its travel throughout the chamber. That the spread of this dark cloud is not exactly in the form of a high-speed flame propagation, however, is seen from a frame-by-frame examination of the pic-

tures. In an examination of frames B-1 to C-1, it will be seen that the dark cloud never has a sharply defined front and it will be observed that several dark regions develop ahead of the advancing cloud and are overtaken by it. The average speed of the advancing cloud, determined by the method explained in reference 5, taking the focal-plane-shutter effect of the camera into account, is 1900 feet per second.

The authors have concluded from their study of frames B-1 to C-1 of figure 13 that the wild flame traveling through the combustion chamber in these frames at a speed of 1900 feet per second is actually a borderline case between homogeneous autoignition and a detonation wave. The speed of 1900 feet per second is in the neighborhood of the speed of sound in the unignited gas, but less than the speed of sound in the fully burned gas. Apparently at the time this wild flame propagated throughout the chamber, the entire chamber contents were ready to undergo homogeneous autoignition. Conditions being, by chance, very slightly more severe in the immediate vicinity of the flame proceeding from the spark plug in B position, the homogeneous autoignition started first in this position. The increased temperature and the compression of the adjacent gases by the autoigniting gases in the vicinity of the spark plug in B position served to spread the autoignition progressively from this position. The fact that the autoignition could spread in this manner, at a speed approximating the speed of sound in the autoigniting gases and with a very diffuse propagation front, may indicate a moderate rate of heat release during the early stages of autoignition as compared with the rate of heat release in the front of a detonation wave.

Upon examination of frames C-1 and C-2 of figure 13 it will be seen that the over-all appearance of frame C-1 is one of dark mottling, whereas the over-all appearance of frame C-2 is fairly white. In reference 5 it is shown that a uniform change throughout the entire area of the picture, occurring between one frame and the next, was explained by a spatially progressive change traveling across the picture in the direction from the previously taken frames toward the later-taken frames at a speed approximating the speed of the focal-plane shutter of the camera. In the case of figure 13 the ratio of image size on the original film to the actual size of the combustion chamber was 0.0342 and the speed of the focal-plane shutter on the film was 251 feet per second. The fairly uniform change throughout the entire area of frame C-2 relative to frame C-1 therefore indicates that the whitening of the field of view traveled across frame C-2 from left to right at a speed of about 7500 feet per second referred to actual combustion-chamber scale. It may therefore be concluded that a detonation wave traveled across the combustion chamber during the exposure of frame C-2 approximately in the opposite direction to the travel of the wild flame in frames B-1 to C-1 and at a rate of about 7500 feet per second. This speed is of the same order as knocking detonation-wave speeds of 6500 feet per second and 6800 feet per second determined in references 5 and 7, respectively.

Careful comparison of frames B-7 and C-1 indicates that the wild flame has completed its travel throughout all parts of the combustion chamber before the exposure of frame C-1. In frame B-7 the flame from the spark plug in position E appears sharply defined. In frame C-1 this flame is no longer so sharply defined, an indication that the wild flame from the B position has begun to merge with the flame from the E position in frame C-1. It appears, therefore, as has

been observed in references 3, 4, 5, and 7 that the knocking reaction probably originates in previously inflamed gases.

The pressure-time trace corresponding to figure 13 is shown in figure 14. The knock occurred quickly after the time of spark ignition and before any perceptible rise in pressure due to normal combustion had taken place. Considering the time of knock to correspond with frame C-2, the vertical line marked "beginning of autoignition" in figure 14 corresponds to the start of the wild flame propagation in frame B-1. The rapid rise in pressure between the vertical line and knock is evidently caused by the passage of the wild autoignition flame across the combustion chamber, indicating that this wild autoignition flame actually is a form of combustion releasing a significant amount of heat in the gases. The violent pressure fluctuations beginning at the position designated knock were probably set up by the rapid reaction occurring at frame C-2 of figure 13. (See reference 3.)

**Knock without autoignition.**—Another high-speed motion picture of the combustion of S-4 reference fuel is presented in figure 15. Frame A-1 was exposed about 130 frames after the ignition of the charge at four spark plugs. The flames develop in a perfectly regular manner throughout frames A-1 to F-2 with no sign of either pin-point autoignition or homogeneous autoignition. In frame F-3 the area of the unignited end zone is suddenly diminished by rapid progression of the flame fronts and the mottled zone shows the characteristic blurred appearance, which was previously found to be intimately connected with the inception of the knocking reaction (reference 3). No autoignition is visible in frame F-3. In frame F-4 the mottled zone adjacent to the unignited end gas is obliterated by the knock reaction and the end gas still shows no change. The knock reaction may have consumed the end gas at about the time of exposure of frame F-4, but, if so, the combustion of the end gas must have occurred in a very short time relative to the 25-microsecond period of exposure in frame F-4. If a significant amount of burning had occurred in the end zone, the resulting expansion would have caused an outward motion of the mottled zones bordering the end zone instead of the rapid progression of the mottled zone into the end zone as actually observed. This rapid advancement indicates that the end zone was actually compressed by the rapidly burning gases all around it. In the next frame (F-5) practically all the mottled zone has been eliminated, while subsequent frames show the violent swirling and bouncing of the burned gases caused by the knock.

The pressure-time trace for this combustion cycle is presented in figure 16. The onset of the knocking vibration was extremely abrupt; no peculiarities in the rate of pressure rise prior to the knock can be seen. The knock was violent, as is shown by the fact that the pressure amplitude of the knocking vibration was considerably greater than the total pressure rise caused by the combustion preceding the knock.

The development of knock in the mottled combustion zone without any preceding autoignition of the end gas is clearly shown in figure 15. Chemical reactions undetected

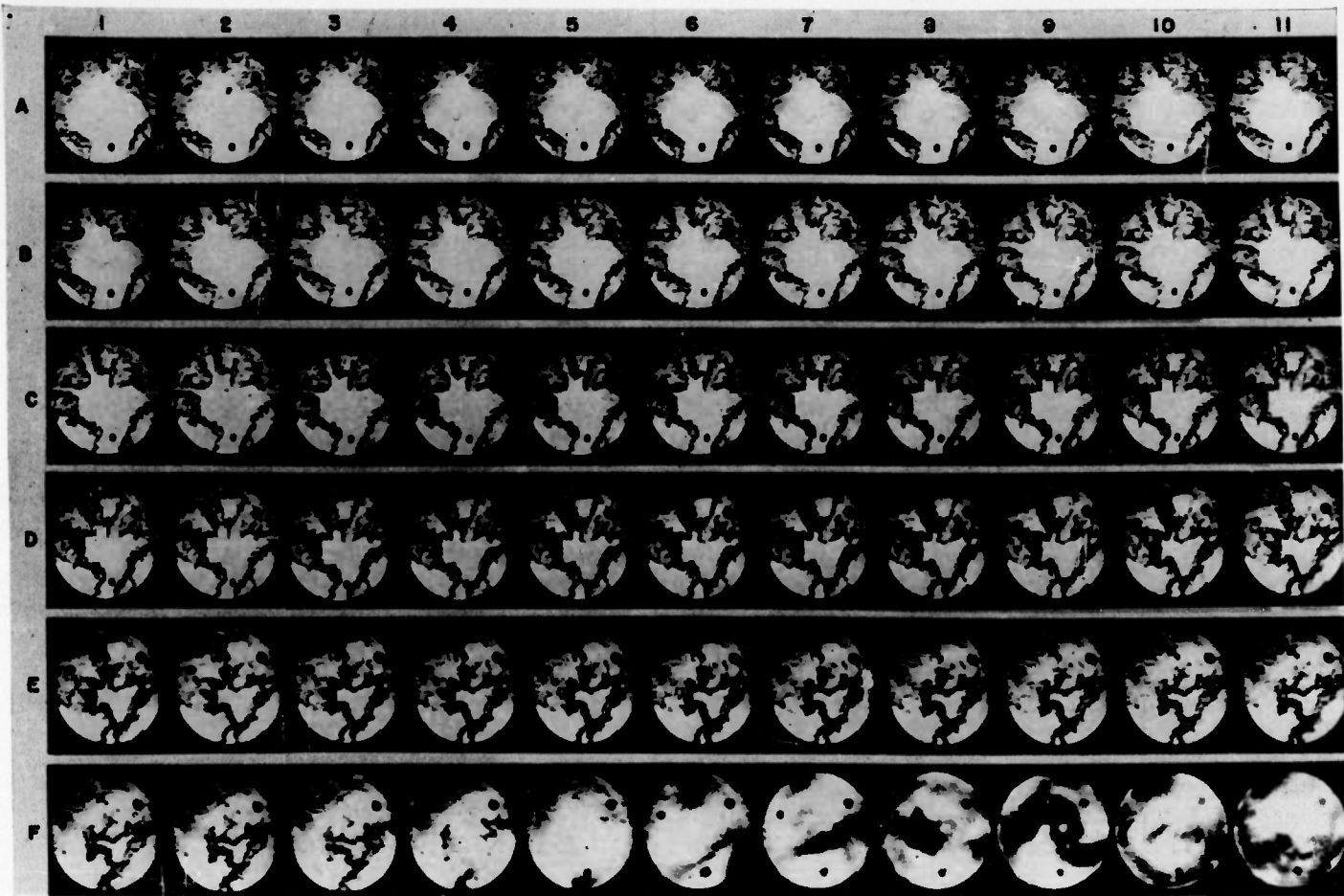


FIGURE 15.—High-speed motion picture of combustion of S-4 reference fuel showing occurrence of violent knock preceded by no autoignition of any kind.

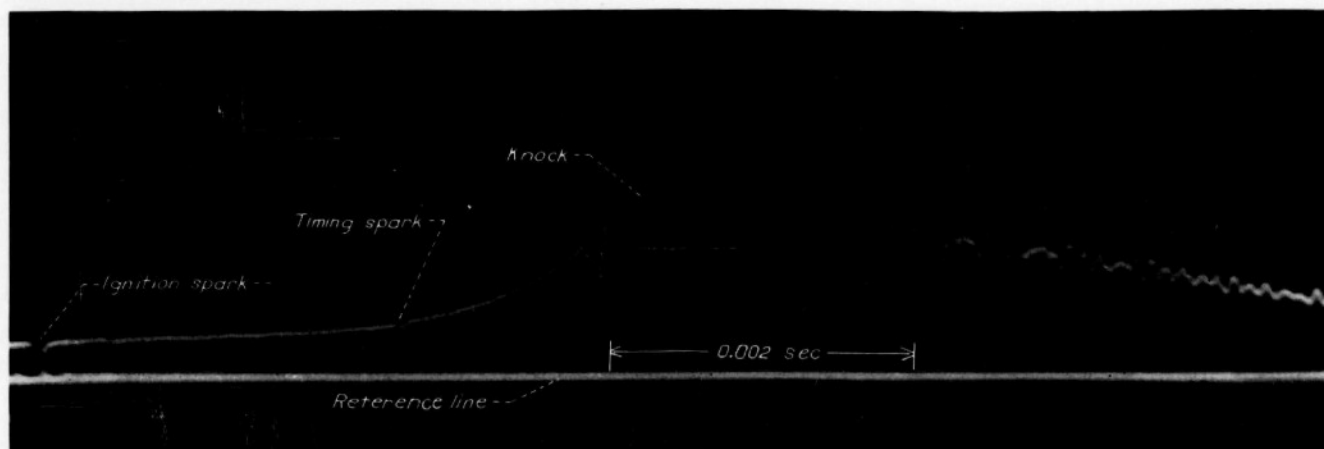


FIGURE 16.—Pressure-time record of combustion of S-4 reference fuel corresponding to figure 15.

by the camera may have occurred in the end zone before the exposure of frame F-3, but if so they released little heat as compared with the autoignitions seen in other figures. The

figure indicates that violent knock can develop in the burning gas independently of any form of end-zone autoignition observable with the test equipment.

**Relation of autoignition to knock.**—As has been shown previously, knock bears about the same relation to pin-point autoignition as it does to the normal burning ignited by sparks. That is to say, knock may or may not occur in the presence of pin-point autoignition, depending mostly upon the nature of the fuel. The engine conditions conducive to the occurrence of pin-point autoignition are also conducive to knock, so that the phenomenon occurring first is determined by the relative propensities of the fuel to autoignite or to knock. Benzene, 2,2,3-trimethylbutane, and S-4 fuels all produce pin-point autoignition at similar engine conditions, but the knocking propensities of these fuels under these same conditions are markedly different. The benzene could not be made to knock at the highest peak compression pressure and inlet-air temperature available. The 2,2,3-trimethylbutane knocked lightly at the most severe conditions available, and the S-4 knocked with extreme violence under similar conditions. Violent knock without the observed occurrence of pin-point autoignition was obtained in the case of S-4 (fig. 15). Pin-point autoignition was observed both with benzene and with 2,2,3-trimethylbutane without any sign of vibratory knock. Pin-point autoignition and knock therefore seem to be completely distinct phenomena either of which may occur independently of the other.

Homogeneous autoignition cannot be so definitely isolated from knock as pin-point autoignition. Violent knock with S-4 fuel involving a large unburned end zone has been observed without any trace of homogeneous autoignition (fig. 15). Almost every case of homogeneous autoignition so far observed with the NACA high-speed camera has been followed by heavy knock. A recent photograph not included in this paper, however, shows homogeneous autoignition without vibratory knock. The extent and duration of homogeneous autoignition before the occurrence of knock has been seen to vary over wide limits. Figure 11 shows a very extensive development of homogeneous autoignition far in advance of the knock. Other records of the combustion of M-4 are on hand in which homogeneous autoignition developed throughout a relatively large end zone no more than one frame before knock occurred. Figure 7 shows the development of homogeneous autoignition in frame E-9 almost simultaneously with the development of knock, but homogeneous autoignition has been observed to occur with S-4 fuel as far as four frames before the knock. Even with the same fuel, violent knock can therefore be produced in the presence of homogeneous autoignition of widely varying extent and stage of development.

In all high-speed photographs in which the origin of knock could be located, the origin has been shown to be in a portion of the charge that appeared already inflamed. (See references 3, 5, and 7.) The homogeneous autoignition, with its rapid development of a large volume of inflamed gas, would seem, therefore, to offer increased opportunity for the knock to occur. Also, the rapid rise in pressure that accompanies the autoignition is conducive to the development of knock. The homogeneous autoignition sets the stage for the knock to take place by rapidly bringing about the conditions favorable to the knocking reaction. It should be noted

again, however, that violent knock may take place in the presence of unburned end zones without any previous signs of autoignition whatsoever. While knock, therefore, does not require the presence of homogeneous autoignition, the development of homogeneous autoignition favors the occurrence of knock.

### CONCLUSIONS

The following conclusions appear justified by the data presented:

1. The knocking reaction has been obtained independently of either observed pin-point autoignition or homogeneous autoignition.
2. Pin-point autoignition may occur independently of the knocking reaction.
3. The knocking reaction may occur at various stages in the development of homogeneous autoignition.
4. High inlet-air temperature and pressure are conducive to the occurrence of both pin-point autoignition and homogeneous autoignition.
5. The occurrence of knock, pin-point autoignition, or homogeneous autoignition under given engine conditions varies greatly with fuel type.

AIRCRAFT ENGINE RESEARCH LABORATORY.

NATIONAL ADVISORY COMMITTEE FOR AERONAUTICS,  
CLEVELAND, OHIO, February 10, 1947.

### REFERENCES

1. Rothrock, A. M., Spencer, R. C., and Miller, Carey D.: A High-Speed Motion-Picture Study of Normal Combustion, Knock, and Preignition in a Spark-Ignition Engine. NACA Rep. No. 704, 1941.
2. Miller, Carey D.: A Study by High-Speed Photography of Combustion and Knock in a Spark-Ignition Engine. NACA Rep. No. 727, 1942.
3. Miller, Carey D., and Olsen, H. Lowell: Identification of Knock in NACA High-Speed Photographs of Combustion in a Spark-Ignition Engine. NACA Rep. No. 761, 1943.
4. Miller, Carey D., and Logan, Walter O., Jr.: Preknock Vibrations in a Spark-Ignition Engine Cylinder as Revealed by High-Speed Photography. NACA Rep. No. 785, 1944.
5. Miller, Carey D.: Relation between Spark-Ignition Engine Knock, Detonation Waves, and Autoignition as Shown by High-Speed Photography. NACA Rep. No. 855, 1946.
6. Sokolik, A., and Voinov, A.: Knocking in an Internal-Combustion Engine. NACA TM No. 928, 1940.
7. Miller, Carey D., Olsen, H. Lowell, Logan, Walter O., Jr., and Osterstrom, Gordon E.: Analysis of Spark-Ignition Engine Knock as Seen in Photographs Taken at 200,000 Frames per Second. NACA Rep. No. 857, 1946.
8. Woodbury, C. A., Lewis, H. A., and Canby, A. T.: The Nature of Flame Movement in a Closed Cylinder. SAE Jour., vol. VIII, no. 3, Mar. 1921, pp. 209-218.
9. Withrow, Lloyd, and Boyd, T. A.: Photographic Flame Studies in the Gasoline Engine. Ind. and Eng. Chem. (Ind. ed.), vol. 23, no. 5, May 1931, pp. 539-547.
10. Miller, Carey D.: The NACA High-Speed Motion-Picture Camera. Optical Compensation at 40,000 Photographs per Second. NACA Rep. No. 856, 1946.
11. Krebs, Richard P., and Dallas, Thomas: Constant-Gain Pickup Amplifier. Electronics, vol. 20, no. 1, Jan. 1947, pp. 87-89.

Reproduced by



CENTRAL AIR DOCUMENTS OFFICE

WRIGHT-PATTERSON AIR FORCE BASE - DAYTON, OHIO

REEL-C

3363 B

A.T.I

71048

*The*  
U.S. GOVERNMENT

IS ABSOLVED

FROM ANY LITIGATION WHICH MAY ENSUE FROM ANY  
INFRINGEMENT ON DOMESTIC OR FOREIGN PATENT RIGHTS  
WHICH MAY BE INVOLVED.

UNCLASSIFIED

ATI- 71 048

NACA, Lewis Flight Propulsion Lab., Cleveland,  
O. (912)

**THE INTERDEPENDENCE OF VARIOUS TYPES  
OF AUTOIGNITION AND KNOCK**, by H. Lowell Olsen,  
and Cearcy D. Miller. 10 Feb '47, 16 pp.

UNCLASSIFIED

(Not abstracted)

**DIVISION:** Power Plants, Reciprocating (6) 27  
**SECTION:** Performance (13) 1.4  
**PUBLISHED BY:** National Advisory Committee for  
Aeronautics  
**DISTRIBUTION:** U.S. Military Organizations request  
copies from ASTIA-DSC. Others route request to  
ASTIA-DSC thru AMC, Wright-Patterson Air Force  
Base, Dayton, O. Attn: NACA.

I. Olsen, H. Lowell  
II. Miller, Cearcy D.

ARMED SERVICES TECHNICAL INFORMATION AGENCY  
DOCUMENT SERVICE CENTER

ATI- 71 048

NACA, Lewis Flight Propulsion Lab., Cleveland,  
O. (912)

**THE INTERDEPENDENCE OF VARIOUS TYPES  
OF AUTOIGNITION AND KNOCK**, by H. Lowell Olsen,  
and Cearcy D. Miller. 10 Feb '47, 16 pp.

UNCLASSIFIED

(Not abstracted)

**DIVISION: Power Plants, Reciprocating (6)**

**SECTION: Performance (13)**

**PUBLISHED BY: National Advisory Committee for  
Aeronautics**

**DISTRIBUTION: U.S. Military Organizations request  
copies from ASTIA-DSC. Others route request to  
ASTIA-DSC thru AMC, Wright-Patterson Air Force  
Base, Dayton, O. Attn: NACA.**

I. Olsen, H. Lowell

II. Miller, Cearcy D.

ARMED SERVICES TECHNICAL INFORMATION AGENCY  
DOCUMENT SERVICE CENTER